Molecular Biology of the Cell
Vol. 17, 3197–3210, July 2006

# Distinct Mechanisms of Clathrin-independent Endocytosis Have Unique Sphingolipid Requirements[D]

**Zhi-Jie Cheng,* Raman Deep Singh,* Deepak K. Sharma,*† Eileen L. Holicky,* Kentaro Hanada,‡ David L. Marks,* and Richard E. Pagano***

*Department of Biochemistry and Molecular Biology, Thoracic Diseases Research Unit, Mayo Clinic College of Medicine, Rochester, MN 55905; and ‡Department of Biochemistry and Cell Biology, National Institute of Infectious Diseases, Tokyo 162-8640, Japan

Submitted December 5, 2005; Accepted April 24, 2006

**Sphingolipids (SLs) play important roles in membrane structure and cell function. Here, we examine the SL requirements of various endocytic mechanisms using a mutant cell line and pharmacological inhibitors to disrupt SL biosynthesis. First, we demonstrated that in Chinese hamster ovary cells we could distinguish three distinct mechanisms of clathrin-independent endocytosis (caveolar, RhoA, and Cdc42 dependent) which differed in cargo, sensitivity to pharmacological agents, and dominant negative proteins. General depletion of SLs inhibited endocytosis by each clathrin-independent mechanism, whereas clathrin-dependent uptake was unaffected. Depletion of glycosphingolipids (GSLs; a subgroup of SLs) selectively blocked caveolar endocytosis and decreased caveolin-1 and caveolae at the plasma membrane. Caveolar endocytosis and PM caveolae could be restored in GSL-depleted cells by acute addition of exogenous GSLs. Disruption of RhoA- and Cdc42-regulated endocytosis by SL depletion was shown to be related to decreased targeting of these Rho proteins to the plasma membrane and could be partially restored by exogenous sphingomyelin but not GSLs. Both the in vivo membrane targeting and in vitro binding to artificial lipid vesicles of RhoA and Cdc42 were shown to be dependent upon sphingomyelin. These results provide the first evidence that SLs are differentially required for distinct mechanisms of clathrin-independent endocytosis.**

## INTRODUCTION

In recent years, several clathrin-independent mechanisms of endocytosis have been identified in mammalian cells. The protein machinery supporting these various endocytic mechanisms and appropriate markers for distinguishing these pathways are just beginning to be defined (Smart *et al*., 1999; Nichols and Lippincott-Schwartz, 2001; Johannes and Lamaze, 2002; Sabharanjak *et al*., 2002; Parton and Richards, 2003). One well studied nonclathrin mechanism is uptake via caveolae—flask-shaped invaginations at the plasma membrane (PM) that are enriched in sphingolipids (SLs), cholesterol (Chol), and caveolin-1 (Cav1) (Mineo and Anderson, 2001; Parton, 2003). Caveolae have been shown to be involved in the uptake of certain viruses (e.g., simian virus 40 [SV40]), toxins (e.g., cholera toxin B subunit [CtxB]), bacteria, and albumin (Orlandi and Fishman, 1998; Lencer *et al*., 1999; Shin *et al*., 2000; Norkin, 2001; Pelkmans *et al*., 2001; Richterova *et al*., 2001; Duncan *et al*., 2002; Marjomaki *et al*., 2002; Minshall *et al*., 2002; Singh *et al*., 2003).

Our laboratory has demonstrated that the fluorescent SL analog BODIPY-lactosylceramide (BODIPY-LacCer) is internalized via caveolae in a range of cell types (Puri *et al*., 2001; Singh *et al*., 2003). BODIPY-LacCer is internalized rapidly and can be observed within Cav1-positive vesicles by 1–2 min after initiation of endocytosis at 37°C (Puri *et al*., 2001; Singh *et al*., 2003, 2004). In human skin fibroblasts, BODIPY-LacCer is delivered to early endosomes within 5–10 min of internalization, and eventually a portion reaches the Golgi apparatus (Puri *et al*., 2001; Choudhury *et al*., 2002; Sharma *et al*., 2003). The uptake by caveolae and subsequent trafficking of BODIPY-LacCer is considerably different from that reported for SV40 virus, which is internalized much more slowly, does not enter early endosomes, and is delivered to the ER without passage through the Golgi apparatus (Pelkmans *et al*., 2001). It is unknown whether BODIPY-LacCer and SV40 virus are internalized by identical mechanisms, and the possibility that there are multiple forms of caveolar endocytosis has been discussed (Le and Nabi, 2003).

Other clathrin-independent uptake mechanisms involve membrane microdomains that have a similar lipid composition to caveolae but that are devoid of caveolins (Damm *et al*., 2005; Kirkham *et al*., 2005b). These include 1) the uptake of the interleukin 2 receptor (IL-2R) by a clathrin-independent, dynamin (Dyn)- and RhoA-dependent mechanism (Lamaze *et al*., 2001; Sabharanjak *et al*., 2002); and 2) uptake of some glycosylphosphatidylinositol (GPI)-anchored proteins as well as fluorescent dextrans via a clathrin- and Dyn2-independent, Cdc42-regulated pinocytic pathway (Sabharanjak *et al*., 2002). Although several studies have demonstrated the existence of multiple nonclathrin endocytic pathways with different cargo, protein machinery, and pharmacological sensitivities within a single cell type (Sabharanjak *et al*., 2002; Singh *et al*., 2003; Sharma *et al*., 2004), the distinction between the various clathrin-independent pathways is not al-

This article was published online ahead of print in *MBC in Press* (http://www.molbiolcell.org/cgi/doi/10.1091/mbc.E05–12–1101) on May 3, 2006.

[D] The online version of this article contains supplemental material at *MBC Online* (http://www.molbiolcell.org).

† Present address: Photometrics, 3440 East Britannia Dr., Tucson, AZ 85706.

Address correspondence to: Richard E. Pagano (pagano.richard@mayo.edu).

ways clear. For example, the use of cholesterol sequestering (e.g., nystatin or filipin) or extracting agents (e.g., cyclodextrins) may not differentiate between uptake via caveolae or other cholesterol-dependent mechanisms (Orlandi and Fishman, 1998; Singh *et al*., 2003). In addition, endocytic markers may behave differently in varying cell types. For example, CtxB may be internalized via caveolae, clathrin-mediated endocytosis, or other mechanisms depending on cell type (Orlandi and Fishman, 1998; Torgersen *et al*., 2001; Singh *et al*., 2003). Finally, the caveolar markers SV40 and CtxB are internalized via caveolae-independent mechanisms in both wild-type and Cav1 knockout mouse embryonic fibroblasts (Damm *et al*., 2005; Kirkham *et al*., 2005b).

Interestingly, markers for clathrin-independent endocytosis are often found in PM microdomains (Brown and London, 1998; Sabharanjak *et al*., 2002; Nabi and Le, 2003; Parton and Richards, 2003; Simons and Vaz, 2004), suggesting that SLs and cholesterol might play a role in the regulation of these endocytic mechanisms. Indeed, endocytosis of SLs, GPI-anchored proteins, albumin, SV40, and CtxB are reported to be sensitive to cholesterol depletion or sequestration (Orlandi and Fishman, 1998; Pelkmans *et al*., 2002; Sabharanjak *et al*., 2002; John *et al*., 2003; Singh *et al*., 2003). We recently found that addition of exogenous glycosphingolipids (GSLs) selectively stimulates caveolar-mediated endocytosis (Sharma *et al*., 2004), suggesting a regulatory role for SLs in this process. However, only a few studies have dealt with the role of SLs in endocytosis in mammalian cells or in yeast (Chen *et al*., 1995; Zanolari *et al*., 2000), and it is unknown whether any of the clathrin-independent endocytic mechanisms specifically requires SLs for normal function.

In the current study, we used a mutant Chinese hamster ovary (CHO) cell line (SPB-1 cells) (Hanada *et al*., 1990) deficient in SL biosynthesis at the nonpermissive temperature as well as selective inhibitors of SL synthesis (Supplemental Figure 1) to dissect the requirement of various endocytic mechanisms for different SLs. We show that 1) general depletion of SLs inhibits multiple mechanisms of clathrin-independent endocytosis but not clathrin-dependent uptake; 2) depletion of GSLs selectively inhibits caveolar endocytosis; and 3) overall depletion SLs inhibits clathrin-independent endocytic mechanisms involving RhoA or Cdc42, because of the loss of sphingomyelin (SM), which is required for their translocation to the PM. These findings provide the first evidence that SLs are differentially required by multiple mechanisms of clathrin-independent endocytosis.

## MATERIALS AND METHODS

### *Lipids and Miscellaneous Reagents*

BODIPY-LacCer was synthesized as described previously (Martin and Pagano, 1994). C8-ceramide and monosialoganglioside $GM_3$ were from Matreya (State College, PA). *N*-hexanoyl sphingosylphosphorylcholine (C6-sphingomyelin; C6-SM), phosphatidylcholine (1,2-dimyristoyl-sn-glycero-3-phosphocholine; DMPC), D-lactosyl-β1-1′-*N*-octanol-D-erythro-sphingosine (C8-LacCer), and bovine brain SM were from Avanti Polar Lipids (Alabaster, AL). Fluorescent Alexa Fluor AF594- or AF647-labeled albumin, transferrin (Tfn), and dextran were from Invitrogen (Carlsbad, CA); and DiI-LDL was from Intracel (Frederick, MD). Tyrosine kinase inhibitor PP2 was from Calbiochem (San Diego, CA). Cholesterol, *Clostridium difficile* toxin B, and FB1 were from Sigma-Aldrich (St. Louis, MO). *N*-butyldeoxygalactonojirmycin (NB-DGJ) was from Toronto Research Chemicals (Toronto, Ontario, Canada). D,L-*threo*-1-Phenyl-2-hexadecanoylamino-3-pyrrolidino-1-propanol (PPPP) was gift from Dr. J. Shayman (University of Michigan, Ann arbor, MI). The IL-2R β chain antibody mik-β3, labeled with phycoerythrin (PE), and anti-PM-Cav1 (C43420) and anti-Golgi-Cav1 (C37120) were from BD Biosciences PharMingen (San Diego, CA). Plasmids encoding the IL-2R β chain (IL-2R β) (A. Dautry-Varsat, Institut Pasteur, Paris, France), DN AP180 (H. McMahon, MRC Laboratory of Molecular Biology, University College London, London, United Kingdom), and Dyn2 K44A (M. McNiven, Mayo Foundation, Rochester, MN), and wild-type (WT), constitutively active (CA), and dominant negative (DN) RhoA and Cdc42 (in pcDNA3.1) (D. Billadeau, Mayo Foundation) were generous gifts as noted. Green fluorescent protein (GFP)-RhoA Q63L and GFP-Cdc42 Q61L were generated by subcloning into the enhanced green fluorescent protein (EGFP)-C3 vector (Clontech, Mountain View, CA) at the HindIII and ApaI sites. HA-Rho and HA-Cdc42 were from the University of Missouri cDNA Resource Center (Rolla, MO). Cav1-monomeric red fluorescent protein (mRed) was generated as described previously (Sharma *et al*., 2004).

### *Lipid Analysis*

Lipid extraction and analysis were performed as described previously (Puri *et al*., 2003). SLs were separated by TLC and identified by comparison to known standards using $CHCl_3/CH_3OH$/15 mM $CaCl_2$ [65:35:8 (vol/vol/vol)] as the developing solvent. Primulin was used as a detection reagent, and lipids were quantified by scanning densitometry.

### *RhoA and Cdc42 Activity Assay*

RhoA and Cdc42 activities were determined using commercial kits (RhoA activation kit; catalog no. BK036, Cytoskeleton, Denver, CO; Cdc42 activation kit; catalog no. 17-286) from Upstate Biotechnology, Charlottesville, VA). For both assays, serum-starved cells were incubated in Ham's F-12 with 10% serum for 10 min, chilled on ice, and washed once with phosphate-buffered saline. For RhoA activity, cells were lysed in 500 μl of lysis buffer (50 mM Tris, pH 7.2, 1% Triton X-100, 0.5% sodium deoxycolate, 0.1% SDS, 500 mM NaCl, 10 mM $MgCl_2$, 10 μg/ml each of aprotinin and leupeptin, and 1 mM phenylmethylsulfonyl fluoride (PMSF). Lysates were centrifuged, equal volumes were incubated with the glutathione *S*-transferase (GST)-Rho binding domain of Rhotekin RBD beads (20 μg protein/sample) for 1 h at 4°C, washed three times, and eluted with SDS sample buffer. Bound RhoA was analyzed by SDS-PAGE separation on a 12% polyacrylamide gel, followed by immunoblotting with a monoclonal antibody against RhoA (catalog no. BK036, Cytoskeleton). For Cdc42 activity, cells were lysed in lysis buffer (23 mM HEPES, pH 7.5, 150 mM NaCl, 1% Igepal CA-630, 10 mM $MgCl_2$, 1 mM EDTA, 2% glycerol, and 10 μg/ml each of aprotinin and leupeptin). Cleared lysates were incubated with 20 μg of GST-p21-binding domain of PAK1 for 45 min at 4°C, washed three times, and eluted with SDS sample buffer. Bound Cdc42 was analyzed by Western blotting as described above, using a monoclonal anti-Cdc42 antibody (catalog no. 17-286, Upstate Biotechnology).

### *Cell Culture and Transfection*

The CHO mutant SPB-1, which is defective in serine palmitoyltransferase (SPT) activity, and parental CHO-K1 cells were maintained as described previously (Hanada *et al*., 1990). SPB-1 SLs were depleted by growth in Nutridoma-BO for 2 d at 39°C. SL levels were decreased in CHO-K1 cells by incubation with 20 μg/ml FB1, 100 μM NB-DGJ, or 0.5 μM PPPP for 2 d in culture. Cells were transfected with IL-2R β, Cav1-mRed, GFP-RhoA Q63L, or GFP-Cdc42 Q61L or cotransfected with CFP-Nuc and RhoA T19N, Cdc42 T17N, DN AP180, or Dyn2 K44A using FuGENE 6.

### *Incubation of Cells with Fluorescent Lipids and Various Markers*

BODIPY-LacCer and other nonfluorescent exogenous SLs were complexed to defatted bovine serum albumin (BSA) (Martin and Pagano, 1994). Cells were typically incubated for 30 min at 10°C with 1 μM BODIPY-LacCer/BSA in HEPES-buffered minimal essential medium (HMEM) with glucose, washed twice, and further incubated for the indicated times (usually 3 min) at 37°C. BODIPY-LacCer remaining at the PM was then removed by back-exchange at 10°C as described previously (Martin and Pagano, 1994). For labeled proteins, cells were preincubated with 5 μg/ml AF594-Tfn or 50 μg/ml AF594 or AF647-albumin for 30 min at 10°C, further incubated at 37°C for 5 min or as indicated, and then acid-stripped to remove labeled protein remaining at the cell surface. For fluid phase uptake, cells were incubated with 1 mg/ml AF594-dextran for 5 min at 37°C without preincubation or acid stripping. For IL-2R β internalization, cells transiently transfected with IL-2R β were incubated with 1 nM IL-2 and 5 μg/ml PE-mik-β3 for 5 min at 37°C.

### *Inhibitor Treatments*

Cells were preincubated in HMEM containing 10 nM PP2 or 100 μM *C. difficile* toxin B for 1 h at 37°C, or with 50 μM genistein, 8 μg/ml CPZ, or 5 mM methyl-β-cyclodextrin (mβ-CD) for 30 min at 37°C as described previously (Puri *et al*., 2001; Sharma *et al*., 2004). Inhibitors were present in all subsequent steps of the experiments.

### *Addition of Exogenous Lipids and SMase Treatment*

Cells were preincubated in HMEM containing 20 μM defatted BSA complex with nonfluorescent lipids (C8-ceramide, C6-SM, $GM_3$, and C8-LacCer) for 30 min at 10°C before incubation with various markers as described above. To deplete SM, cells were treated with 200 mU/ml SMase from *Bacillus aureus* (Sigma-Aldrich) at 37° for 2 h.

### *Subcellular Fractionation, RhoA and Cdc42 Translocation*

Cells were fractionated as described previously (del Pozo *et al.*, 2004). Briefly, cells were lysed in ice-cold hypotonic lysis buffer (10 mM HEPES, pH 7.5, 1.5 mM $MgCl_2$, 5 mM KCl, 1 mM dithiothreitol, 0.2 mM sodium vanadate, 1 mM PMSF, and 1 $\mu$g/ml each of aprotinin and leupeptin) for 5 min. Lysates were homogenized and then centrifuged at 700 $\times$ *g* for 3 min. The resulting supernatants were spun at 40,000 $\times$ *g* for 30 min at 4°C to separate the crude membrane pellet (P) from the supernatant (S) containing the cytosol. Ten percent of the membrane fractions and 2% of the cytosol fractions were analyzed by Western blotting using antibodies against RhoA or Cdc42, and quantified by densitometry.

### *Binding of RhoA and Cdc42 to Multilamellar Lipid Vesicles (MLVs)*

Stock solutions of DMPC, cholesterol, and SM in $CHCl_3$ were mixed in various proportions and dried under a stream of nitrogen. Samples were vortex mixed in PPE buffer (5 mM PIPES, 50 mM KCl, and 1 mM EDTA) and further incubated for 30 min at 37°C followed by centrifugation for 15 min at 40,000 $\times$ *g* (4°C). The resulting MLVs were resuspended in PPE buffer at a final concentration of 10 mM lipid. HA-tagged Rho-GTPases were prepared from CHO-K1 cells transiently transfected with HA-RhoA or HA-Cdc42. After 48 h, the HA-tagged proteins were immunoprecipitated from cells lysates using immobilized anti-HA antibody matrix (catalog no. 11815016001; Roche Diagnostics, Indianapolis, IN). Purified HA-RhoA or HA-Cdc42 was loaded with GDP or guanosine 5′-*O*-(3-thio)triphosphate (GTP$\gamma$S) (del Pozo *et al.*, 2004), and 1 $\mu$g of immunoprecipitated protein was incubated with 200 $\mu$M MLVs in 1 ml of PPE buffer for 30 min at 30°C. The samples were then centrifuged and washed twice as described above and resuspended in SDS sample buffer. Bound proteins were detected by immunoblotting using anti-HA or anti-Rho-GDI antibodies.

### *Fluorescence and Electron Microscopy (EM) Studies*

Epifluorescence and total internal reflection fluorescence (TIRF) microscopy were carried out using an Olympus IX70 microscope with an Olympus TIRF module. Quantitation of images was performed using the MetaMorph image-processing program (Molecular Devices, Sunnyvale, CA) as described previously (Sharma *et al.*, 2005). For these studies, whole cell fluorescence was determined by drawing borders around individual cells, and noncellular background was subtracted. All photomicrographs in a given experiment were exposed and processed identically for a given fluorophore. For colocalization studies, no "cross-over" between microscope channels was observed at the concentration and exposure setting used.

For EM studies, cells were grown on Aklar sheets placed in 35-mm culture dishes and were either untreated (control) or incubated with NB-DGJ for 48 h (see above). Samples were fixed in the presence of 1 mM ruthenium red and embedded as described previously (Henley *et al.*, 1998). Transverse ultrathin sections were cut and viewed under a FEI Tecnai T12 transmission electron microscope operating at ~80 kV. Overlapping images of the entire cell perimeter in a given field were taken at 21,000$\times$ magnification. For quantitation, the number of ruthenium red positive, 50- to 80-nm-diameter vesicles within 0.5 $\mu$m of the cell surface were counted for the entire cell perimeter. Values are expressed per 100 $\mu$m of perimeter length.

## RESULTS

### *Clathrin-independent Endocytosis in CHO Cells*

To investigate the role of SLs in endocytosis, we first studied the uptake of the transferrin (Tfn) receptor, a fluorescent GSL analog (BODIPY-LacCer), albumin, IL-2R, and dextran, markers previously shown to internalize by a variety of endocytic mechanisms in CHO cells and other cell types (Sabharanjak *et al.*, 2002; Singh *et al.*, 2003; Sharma *et al.*, 2004).

To monitor caveolar endocytosis, we used BODIPY-LacCer, which is rapidly internalized via caveolae in several cell types, as shown by sensitivity to a range of pharmacological agents and DN proteins (Puri *et al.*, 2003; Singh *et al.*, 2003; Sharma *et al.*, 2004, 2005). Here, we found that BODIPY-LacCer uptake by CHO cells was inhibited by m$\beta$-CD, genistein, and DN Dyn2 protein expression, but it was unaffected by inhibitors of the clathrin pathway (chlorpromazine and DN AP-180 expression) and the Rho protein-dependent pathways (*C. difficile* toxin B, DN RhoA, and Cdc42 expression) (Figure 1, A and B, Supplemental Figure 2, and

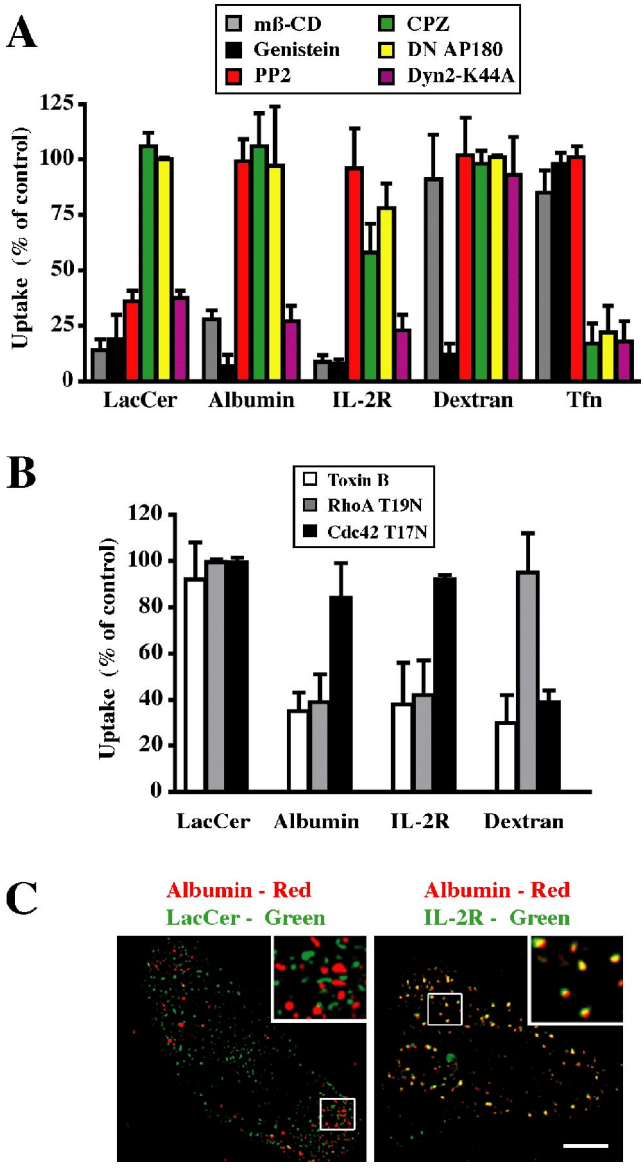


**Figure 1.** Characterization of the endocytosis of various markers in CHO-K1 cells. (A) Cells were pretreated with m$\beta$-CD, genistein, PP2, or CPZ or cotransfected with CFP-Nuc and DN AP180 or Dyn2 K44A constructs. Internalization (5 min at 37°C) of fluorescently labeled LacCer, albumin, dextran, or Tfn, relative to untreated cells (control) was quantified by image analysis. Internalization of IL-2R was followed after transfection of cells with IL-2R $\beta$ (see *Materials and Methods*). (B) Cells were pretreated with toxin B or cotransfected with CFP-Nuc and RhoA T19N or Cdc42 T17N constructs, and internalization (5 min at 37°C) of the indicated marker, relative to that in nontransfected cells, was quantified by image analysis. Values in A and B represent means $\pm$ SD (n $\geq$ 30 from 3 independent experiments). (C) Colocalization of albumin with BODIPY-LacCer versus IL-2R in CHO cells. Cells, untransfected (left) or transfected with IL-2R $\beta$ (right; see *Materials and Methods*), were coincubated with AF647-albumin and either BODIPY-LacCer or PE-mik-$\beta$3. After internalization for 1 min at 37°C, samples were acid stripped and back exchanged before microscopy. Separate images were acquired for each fluorophore, rendered in pseudocolor, and are presented as overlays. Insets show the boxed regions at higher magnification. Note that LacCer and albumin were not colocalized (presence of discrete green and red puncta) whereas LacCer and IL-2R overlapped extensively as shown by the yellow puncta. Bar, 10 $\mu$m.

Supplemental Table 1). In addition, BODIPY-LacCer colocalized with mRed-tagged Cav1 in vesicular structures 1 min after its internalization (Supplemental Figure 3), consistent with our previous studies in other cell types. These data demonstrate that BODIPY-LacCer is internalized via caveolae in CHO cells.

A clear distinction between uptake via caveolae and other nonclathrin pathways was observed using the src family-specific tyrosine kinase inhibitor PP2 (Hanke *et al.*, 1996; Bain *et al.*, 2003). BODIPY-LacCer uptake by CHO cells was strongly inhibited by PP2, whereas IL-2R and dextran (markers for the RhoA- and Cdc42-dependent pathways, respectively) uptake was unaffected by PP2 (Figure 1A and Supplemental Figure 2B). Another feature that differentiated the nonclathrin endocytic pathways was their sensitivity to cholesterol depletion by acute m$\beta$-CD treatment. The uptake of BODIPY-LacCer, IL-2R and albumin was significantly inhibited by treatment with 5 mM m$\beta$-CD (Figure 1A), whereas inhibition of dextran uptake was only observed at higher concentrations (e.g., 15 mM m$\beta$-CD; Supplemental Figure 2A). The limited sensitivity of dextran uptake to cholesterol depletion seems surprising because low doses (4–5 mM) of m$\beta$-CD have been reported to inhibit the uptake and subsequent targeting of cholera toxin in Cav1 knockout cells (Kirkham *et al.*, 2005a) and *Helicobacter pylori* vacuolating toxin in various cell types (Patel *et al.*, 2002; Gauthier *et al.*, 2005). In these studies, both toxins were proposed to be internalized via the Cdc42-dependent mechanism. However, in contrast to dextran, which is a marker for fluid phase uptake, the endocytosis of both toxins requires a membrane binding step and probable association with lipid microdomains before internalization. Thus, one possible explanation for the differences in these studies is that the binding of the toxins to membranes and their organization into microdomains may be more sensitive to cholesterol depletion than the endocytic process itself.

Modified albumins such as fluorescent albumins are internalized via caveolae in some cell types via their binding to cell surface proteins (e.g., gp18 and gp30) (Schnitzer and Oh, 1994; Schnitzer *et al.*, 1994; Singh *et al.*, 2003; Sharma *et al.*, 2004; Bito *et al.*, 2005); however, the mechanism of albumin uptake in CHO cells has not been characterized. We found that albumin endocytosis in CHO cells exhibited properties identical to that of IL-2R, i.e., it was Rho A dependent, tyrosine kinase and Dyn2 dependent, but independent of clathrin and src kinase (Figure 1A and Supplemental Figures 3 and 4; data summarized in Supplemental Table 2). Unlike the uptake of fluorescent dextran, which when used at concentrations of 1 mg/ml is taken up primarily via the fluid phase pathway and is specifically inhibited by DN Cdc42 (Sabharanjak *et al.*, 2002), albumin uptake was selectively inhibited by DN Rho A (Figure 1B and Supplemental Figure 4). Furthermore, albumin colocalized with the IL-2R but not with Cav1-mRed or with the caveolar marker BODIPY-LacCer (Figure 1C and Supplemental Figure 3). Thus, albumin serves as an additional marker for the RhoA-dependent endocytic pathway in CHO cells.

Together, the results in Figure 1, Supplemental Figures 2–4, and Supplemental Table 1 demonstrate that we are able to separately monitor endocytosis via clathrin (Tfn) and three distinct clathrin-independent endocytic mechanisms (caveolar [BODIPY-LacCer], RhoA-dependent [IL-2R and albumin], and Cdc42-dependent [dextran]).

### *SL Depletion Selectively Attenuates Clathrin-independent Endocytosis*

We examined the role of SLs in regulating endocytosis using the temperature-sensitive CHO mutant cell line SPB-1. At the nonpermissive temperature (39°C), these cells fail to synthesize all SLs because of a defect in SPT (Hanada *et al.*, 1990), which catalyzes the first step of SL biosynthesis (refer to Supplemental Figure 1). When SPB-1 and its parental CHO-K1 cells were maintained in 5% fetal bovine serum (FBS) at the permissive temperature (33°C), SPB-1 cells had a similar SL composition to CHO-K1 cells as determined by quantitative lipid analysis of SM and $GM_3$ ganglioside, the two major SLs in CHO cells (Supplemental Table 3). When cultured under nonpermissive conditions, SPB-1 cells exhibited a time-dependent decrease in their SL content, with the maximum reduction (~70–75%), relative to cells cultured under permissive conditions, occurring after 48 h (Supplemental Figure 5A and Supplemental Table 3). In contrast, no significant difference was observed in $GM_3$ ganglioside or SM levels between CHO-K1 cells cultured at 33 or 39°C (Supplemental Table 3).

We then studied the effect of SL depletion on the caveolar endocytosis of BODIPY-LacCer by comparing its initial internalization in SPB-1 versus CHO-K1 cell lines. Cells were incubated with BODIPY-LacCer for 30 min at 10°C to incorporate the lipid into the PM and were then warmed to 37°C to initiate endocytosis. CHO-K1 and SPB-1 cells internalized BODIPY-LacCer to a similar degree when cultured under permissive conditions (Figure 2A). After culture under nonpermissive conditions, SPB-1 cells showed a dramatic reduction in BODIPY-LacCer uptake compared with CHO-K1 cells grown under the same conditions (Figure 2, A and C, and Supplemental Figure 5B), whereas uptake by CHO-K1 cells was unaffected by the culture conditions (Figure 2A). In control experiments, both SPB-1 and CHO-K1 cells cultured under nonpermissive conditions showed similar levels of PM fluorescence after initial incubation with BODIPY-LacCer at 10°C, demonstrating "equal loading" of the PM with BODIPY-LacCer before endocytosis in both normal and SL-depleted cells (Figure 2A, right).

We next examined the initial internalization of other endocytic markers in SPB-1 and CHO-K1 cells under nonpermissive conditions. The uptake of albumin, dextran, and IL-2R, all markers for other clathrin-independent endocytosis, were significantly inhibited in SPB-1 cells, whereas endocytosis of Tfn and DiI-LDL (markers for clathrin-dependent endocytosis) were not affected under the same conditions (Figure 2, B and C). Thus, clathrin-dependent and -independent endocytosis were differentially regulated in this mutant cell line. The extent of reduction in uptake for all the markers of clathrin-independent endocytosis depended on the time in culture at the nonpermissive temperature (Supplemental Figure 5C) and correlated well with the time-dependent change in SL content of SPB-1 cells (Supplemental Figure 5A), suggesting a requirement of SLs for various clathrin-independent endocytic processes.

### *GSL Depletion Selectively Blocks Caveolar Uptake*

Because multiple clathrin-independent mechanisms of endocytosis were inhibited by SL depletion in SPB-1 cells (Figure 2), we next sought to determine whether these mechanisms might be differentially affected by different SL subgroups. For these studies, cells were treated with the ceramide synthase inhibitor fumonisin B1 (FB1) (Merrill *et al.*, 1996), to inhibit both SM and GSLs synthesis, or with glucosylceramide synthase (GCS) inhibitors (NB-DGJ) (Platt

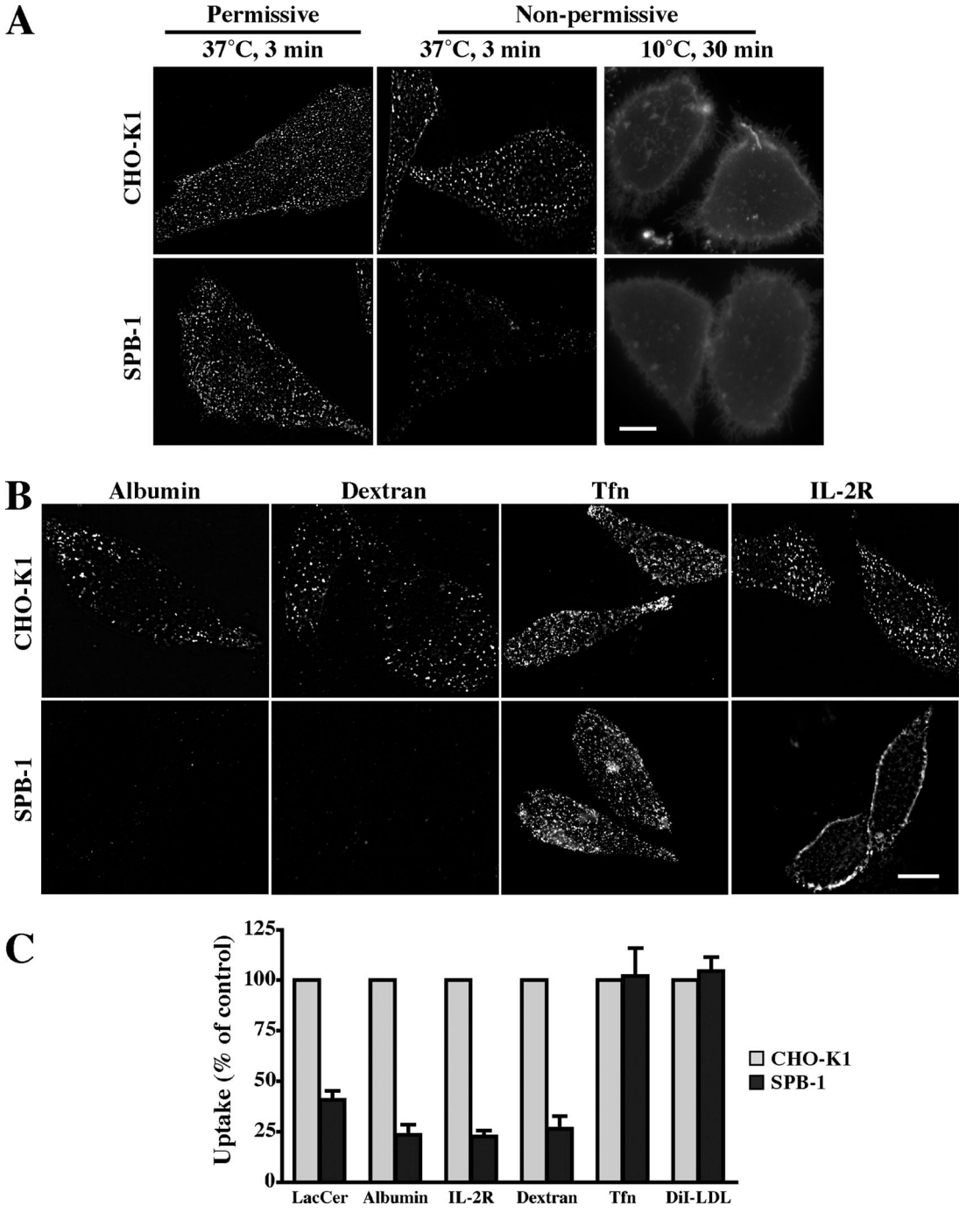


**Figure 2.** SL depletion selectively attenuates clathrin-independent endocytosis. (A) CHO-K1 or SPB-1 cells were cultured under permissive (F-12 medium containing 5% FBS at 33°C; left) or nonpermissive (Nutridoma-BO medium at 39°C; middle and right) conditions for 48 h. Cells were then incubated for 30 min at 10°C with 1 $\mu$M BODIPY-LacCer and immediately observed (right) or warmed for 3 min at 37°C and back exchanged (left, middle) before observation under the fluorescence microscope at green wavelengths. Similar effects were also observed after 5 and 10 min of internalization (Supplemental Figure 5B). (B) CHO-K1 or SPB-1 cells were cultured under nonpermissive conditions for 48 h. Internalization (5 min at 37°C) of the indicated markers was measured as in Figure 1. Bars, 10 $\mu$m. (C) Quantitative analysis of the uptake (5 min at 37°C) of the indicated markers in CHO-K1 and SPB-1 cells cultured under nonpermissive conditions. Results for SPB-1 cells are expressed as percentage of uptake measured in CHO-K1 cells. Values are the mean ± SD (n ≥ 50 cells from 3 independent experiments).

*et al*., 1994) or PPPP (Lee *et al*., 1999), which decreased GSLs and slightly increased SM levels concomitantly (Supplemental Figure 1 and Supplemental Table 4). Using these treatments, we then compared the initial internalization of markers for the various mechanisms of clathrin-independent endocytosis. Treatment with FB1 led to an inhibition of uptake of all the markers for clathrin-independent endocytosis (Figure 3), consistent with our findings using SPB-1 cells (Figure 2), and suggesting a general role for SLs in clathrin-independent endocytosis. In contrast, when cells

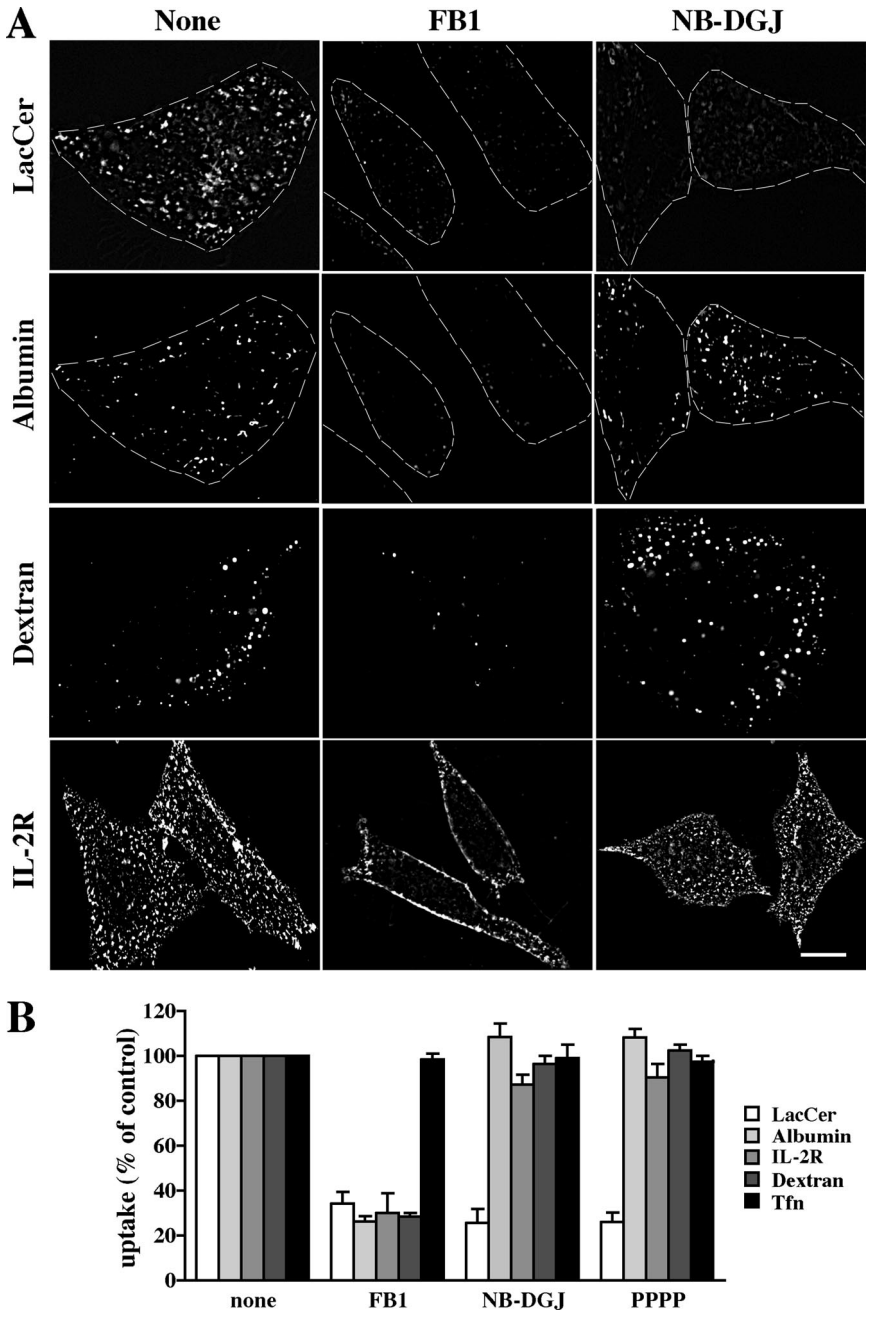


**Figure 3.** GSLs are required for caveolar-mediated endocytosis of BODIPY-LacCer. CHO-K1 cells were pretreated with FB1, NB-DGJ, or PPPP for 48 h (see *Materials and Methods*). The internalization (5 min at 37°C) of BODIPY-LacCer, albumin, dextran, and IL-2R were then observed and quantified as in Figure 1. (A) Representative fluorescence micrographs for control, FB1 or NB-DGJ treated cells. Bar, 10 $\mu$m. (B) Quantitation of marker uptake. Results are expressed as percentage of marker uptake in untreated (control) cells. Values are the mean ± SD (n ≥ 50 cells for each marker).

were treated with either NB-DGJ or PPPP and then double labeled with fluorescent LacCer and albumin, LacCer internalization was inhibited, whereas albumin uptake was unaffected in the same cells. Similarly, no effect was seen on the endocytosis of markers for other clathrin-independent endocytic mechanisms (Figure 3). Based on the biosynthetic steps affected by these inhibitors (Supplemental Figure 1), these results suggest that GSLs are essential for caveolar-mediated endocytosis, whereas other clathrin-independent endocytic mechanisms require SLs other than GSLs (e.g., ceramide or SM).

### *Exogenous SLs Restore Different Mechanisms of Clathrin-independent Endocytosis after SL Depletion*

To specify which SL subgroup (ceramide, SM, or GSLs) was required for particular mechanisms of clathrin-independent endocytosis, we briefly incubated SL-depleted cells with nonfluorescent SLs (C8-ceramide, C6-SM, $GM_3$, or C8-LacCer) and then assessed the effect of these treatments on internalization of BODIPY-LacCer, albumin, IL-2R, and dextran (Figure 4). In these experiments, the incubations with exogenous SLs were carried out at 10°C for short times (30 min) to minimize the subsequent metabolism of these lipids. Uptake of fluorescent LacCer was almost completely rescued by addition of $GM_3$ or nonfluorescent C8-LacCer in cells chronically treated with FB1 (Figure 4, A and C), in agreement with the results in Figure 3, which suggested that GSLs were essential for caveolar-mediated endocytosis. In contrast, C6-SM partially restored albumin, IL-2R, and dextran (but not BODIPY-LacCer) uptake in FB1-treated cells (Figure 4), suggesting that SM was specifically required for Rho-dependent internalization. Addition of C8-ceramide

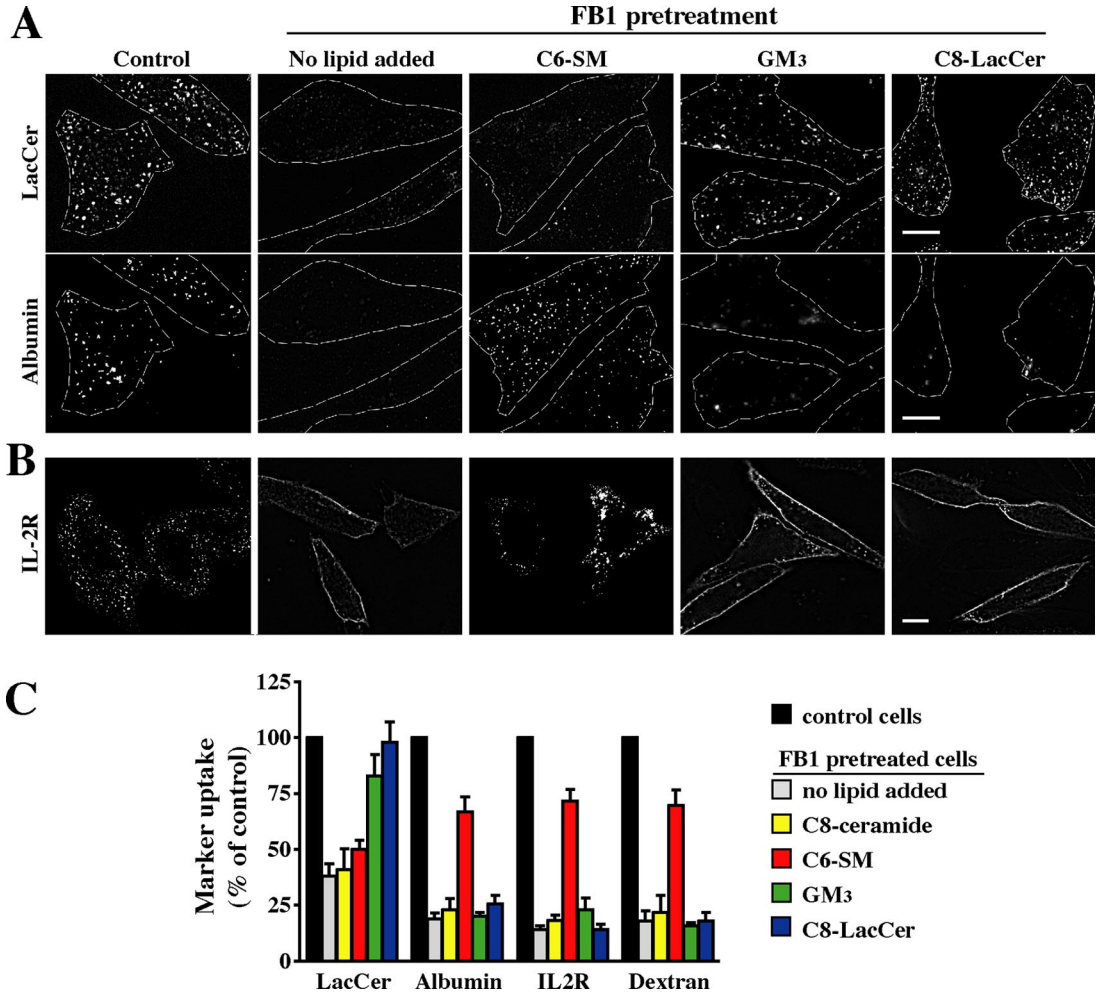


**Figure 4.** Exogenous SLs restore marker uptake in FB1-treated cells. CHO-K1 cells were untreated (control) or pretreated with 20 $\mu$g/ml FB1 for 48 h. FB1-treated cells were then incubated with a 20 $\mu$M BSA complex of C6-SM, $GM_3$, or C8-LacCer for 30 min at 10°C in HMEM. (A) Cells were then double labeled with BODIPY-LacCer and AF647-albumin for 30 min at 10°C, and the internalization (5 min at 37°C) was then measured as described in Figure 1. Dashed lines delineate cell periphery in each field. Bar, 10 $\mu$m. Note that the same fields of cells are shown for LacCer and albumin uptake. (B) Cells were incubated with IL-2R antibody under the same conditions as described in A. Fluorescent regions at the PM indicate noninternalized IL-2R antibody. Bar, 10 $\mu$m. (C) Uptake of BODIPY-LacCer, albumin, IL-2R, or dextran in FB1-treated cells after addition of the indicated exogenous SL. Results were quantified by image analysis and are expressed as a percentage of marker uptake in control cells. Values are the mean ± SD (n ≥ 50 cells for each condition).

had no effect on the endocytosis of any of these markers in SL-depleted cells (Figure 4C).

### *Cav1 and Caveolae in SL-depleted Cells*

To investigate possible mechanisms by which GSL depletion could affect caveolar endocytosis, we examined the intracellular distribution of Cav1 in CHO-K1 cells (±NB-DGJ or ±FB1 treatments) by immunofluorescence using specific Cav1 antibodies and different permeabilization methods previously shown to selectively detect Cav1 pools at the PM or at the Golgi complex (Pol *et al*., 2005). The amount of Cav1 at the PM of CHO-K1 cells treated with NB-DGJ or FB1 was considerably reduced compared with untreated control cells, whereas the Cav1 fluorescence in the Golgi region was dramatically increased (Figure 5, A and B). A loss of Cav1 from the PM upon FB1 or NB-DGJ treatment was also seen using TIRF microscopy in cells overexpressing Cav1-GFP (our unpublished data). In contrast to these results, the total amount of Cav1 present in the cells, detected by Western blotting, was unaffected by these inhibitors (Figure 5B). When FB1-treated cells were incubated with exogenous lipids, the PM localization of Cav1 was restored to the levels seen in control cells untreated with FB1 by addition of C8-lacCer or $GM_3$ but not by C6-SM (Figure 5, E and F). We also analyzed CHO-K1 cells by electron microscopy and found approximately threefold reduction in the number of 50- to 80-nm surface-connected vesicles (presumably caveolae) in cells treated with NB-DGJ relative to untreated control cells (Figure 5, C and D). Incubation of NB-DGJ–treated cells with $GM_3$ restored surface-connected vesicles to the levels seen in untreated cells (Figure 5, C and D).

### *SLs Modulate the Membrane Targeting of Rho GTPases*

RhoA and Cdc42 are members of the Rho GTPase family that are essential for clathrin- and caveolar-independent endocytosis (Sabharanjak *et al*., 2002). In the present study, overexpression of the inactivated, GDP-bound form of RhoA inhibited albumin and IL-2R uptake, whereas the inacti-

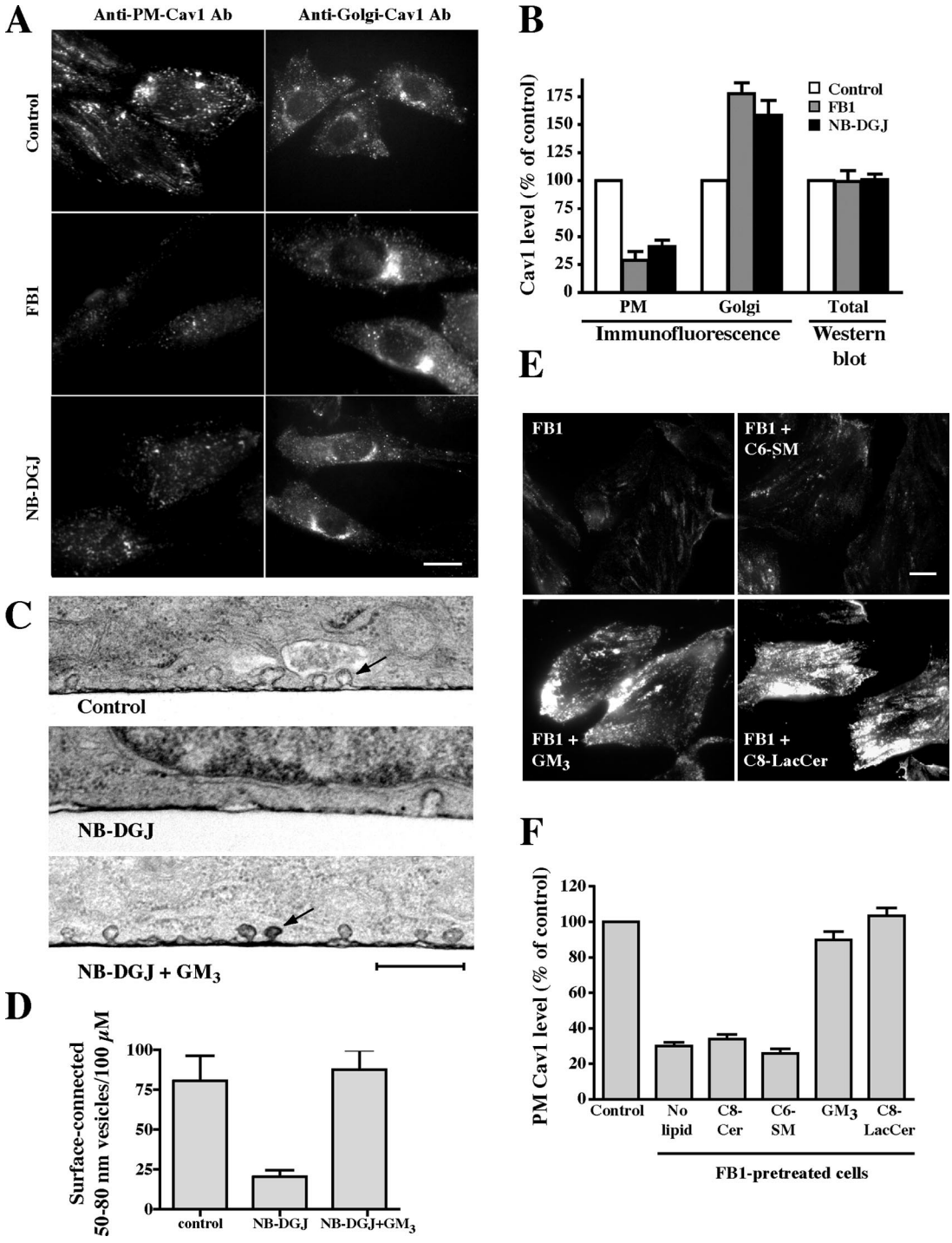


**Figure 5.** Effect of SL depletion on Cav1 distribution and the number of surface-connected, 50- to 80-nm vesicles at the PM of CHO-K1 cells. Cells were untreated (control) or pretreated with FB1 or NB-DGJ for 2 d. (A) Samples were permeabilized with methanol and stained with anti-PM-Cav1 or permeabilized with 0.1% saponin and stained with anti-Golgi-Cav1 antibodies (Pol *et al*., 2005). Cells were then incubated with fluorescent secondary antibodies, and staining was observed by fluorescence microscopy. Bar, 10 $\mu$m. (B) Samples treated and stained for Cav1 as described in A were analyzed for PM (anti-PM-Cav1-antibody) and Golgi (anti-Golgi-Cav1 antibody) Cav1 signal intensity by microscopy and image analysis. Note that the values shown for "Golgi" represent quantitation of entire cell fluorescence detected with the anti-Golgi-Cav1 antibody (see A). No differences in the total amount of Cav1 were detected by Western blotting of cell lysates from control, FB1-, or NB-DGJ–pretreated cells (B). (C andD) Cells were untreated (control), pretreated with NB-DGJ for 48 h, or pretreated with NB-DGJ for 48 h and then with $GM_3$ ganglioside for 30 min at 10°C. Cells were then stained with ruthenium red to identify surface-connected invaginations, fixed, and processed for transmission EM. Samples were sectioned vertically to the substratum. (D) For quantitation, the entire circumference of a given cell in a single section was analyzed. Values represent the number of 50- to 80-nm surface-connected vesicles within 0.5 $\mu$m of the cell surface and are expressed as number per 100 $\mu$m of length. In total, 30 different cells were analyzed for each condition in three independent experiments. Note that the NB-DGJ–treated cells showed approximately threefold reduction in the number of these vesicles per unit length. Bar, 500 nm. (E) Cells treated with FB1 were incubated with exogenous lipids for 30 min at 10°C and then fixed and stained for PM-Cav1

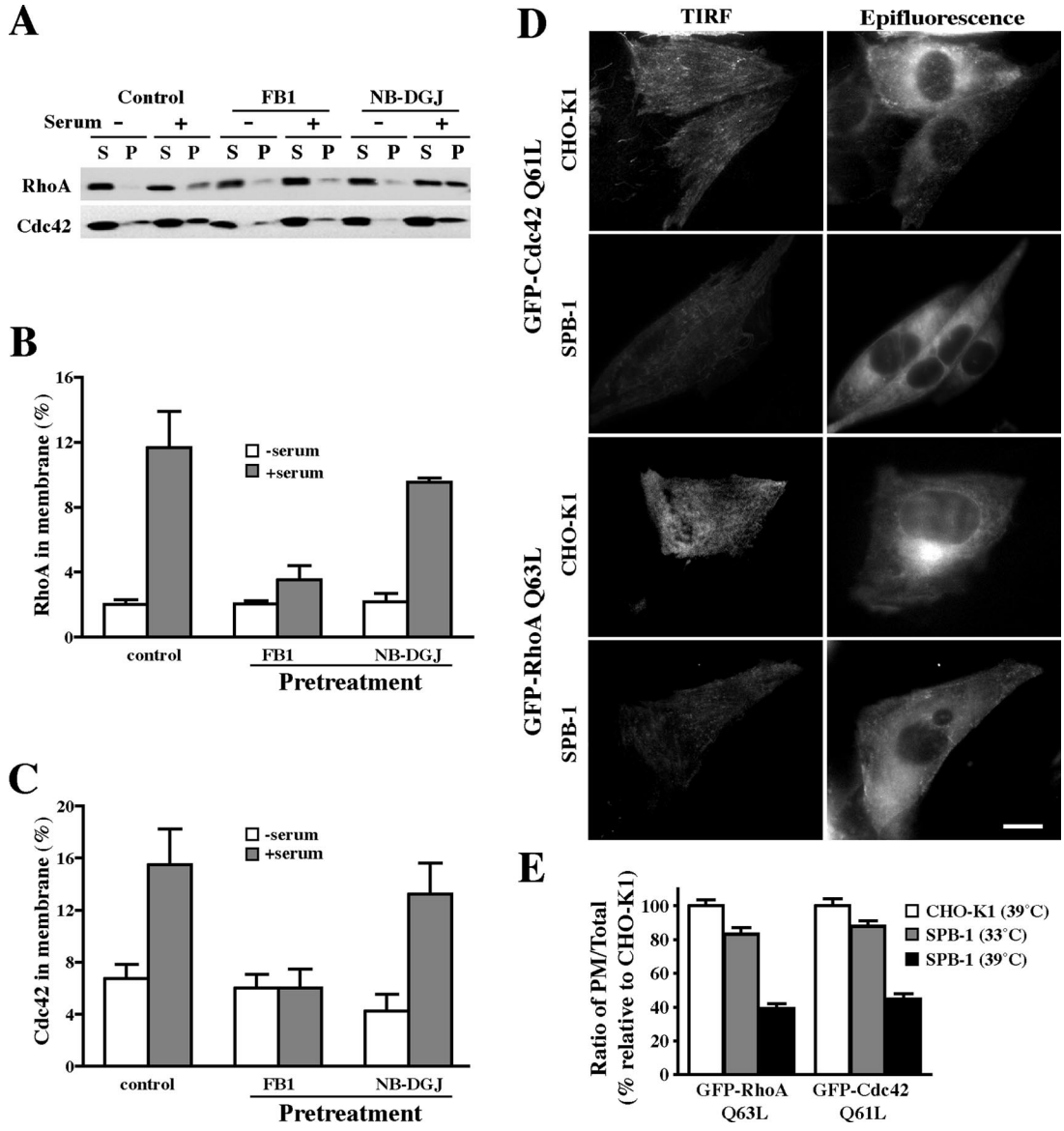


**Figure 6.** SLs modulate the serum-stimulated membrane targeting of Rho GTPases. (A–C) In vitro studies using CHO-K1 cells treated with FB1 or NB-DGJ. (D and E) In situ studies using CHO-K1 and SPB-1 cells. (A) CHO-K1 cells were untreated or pretreated with FB1 or NB-DGJ for 2 d and serum starved overnight. Cells were then stimulated with 10% FBS for 10 min and then lysed in hypotonic buffer. The particulate (P) and soluble (S) fractions were isolated, and 2% of the cytoplasmic fraction and 10% of the membrane fraction were analyzed by Western blotting. (B and C) Densitometric analysis of Rho GTPase translocation to membranes. The percentage of RhoA (B) or Cdc42 (C) in the membrane fraction was calculated accordingly. (D) CHO-K1 and SPB-1 cells transfected with GFP-RhoA Q63L or GFP-Cdc42 Q61L constructs were cultured under nonpermissive conditions for 48 h and then serum starved overnight. The presence of GFP-RhoA Q63L or GFP-Cdc42 Q61L at the PM was observed by TIRF microscopy at 10°C (left). The corresponding cells were also observed by epifluorescence microscopy (right), demonstrating that substantial amounts of GFP fluorescence were present in all the cell samples visualized by TIRF microscopy. Bar, 10 $\mu$m. (E) Quantitative analysis of the PM-associated GFP-RhoA or -Cdc42 in CHO-K1 and SPB-1 cells. SPB-1 cells were evaluated after growth under permissive (33°C) or nonpermissive (39°C; SL-depleted) conditions. Values of PM and total cell fluorescence of individual cells were obtained by image analysis of TIRF and epifluorescence micrographs, respectively, acquired under standardized exposure conditions. PM/total cell fluorescence ratios calculated for SBP-1 cells are expressed relative to ratios for CHO-K1 cells, which were arbitrarily set to 100. Results are the mean ± SD from at least 50 measurements for each condition.

vated form of Cdc42 inhibited dextran internalization (Figure 1B and Supplemental Figure 4). Because exogenously supplied SM (but not other SLs) restored uptake of albumin and dextran in FB1 treated cells (Figure 4), we next examined the mechanism by which this might occur. We first studied the activation of RhoA and Cdc42 in control, FB1-, or NB-DGJ–treated cells and found that serum stimulated GTP loading of either GTPase to similar levels in control, FB1-, or NB-DGJ–treated cells (Supplemental Figure 6), suggesting that SL depletion did not affect their GTP loading. Additional

**Figure 5 (cont).** immunofluorescence as described in A. Bar, 10 $\mu$m. (F) Quantitation of PM labeling in cells treated with FB1 plus exogenous lipids as described in E. Results are means ± SE for ≥30 cells from three independent experiments for each condition shown.

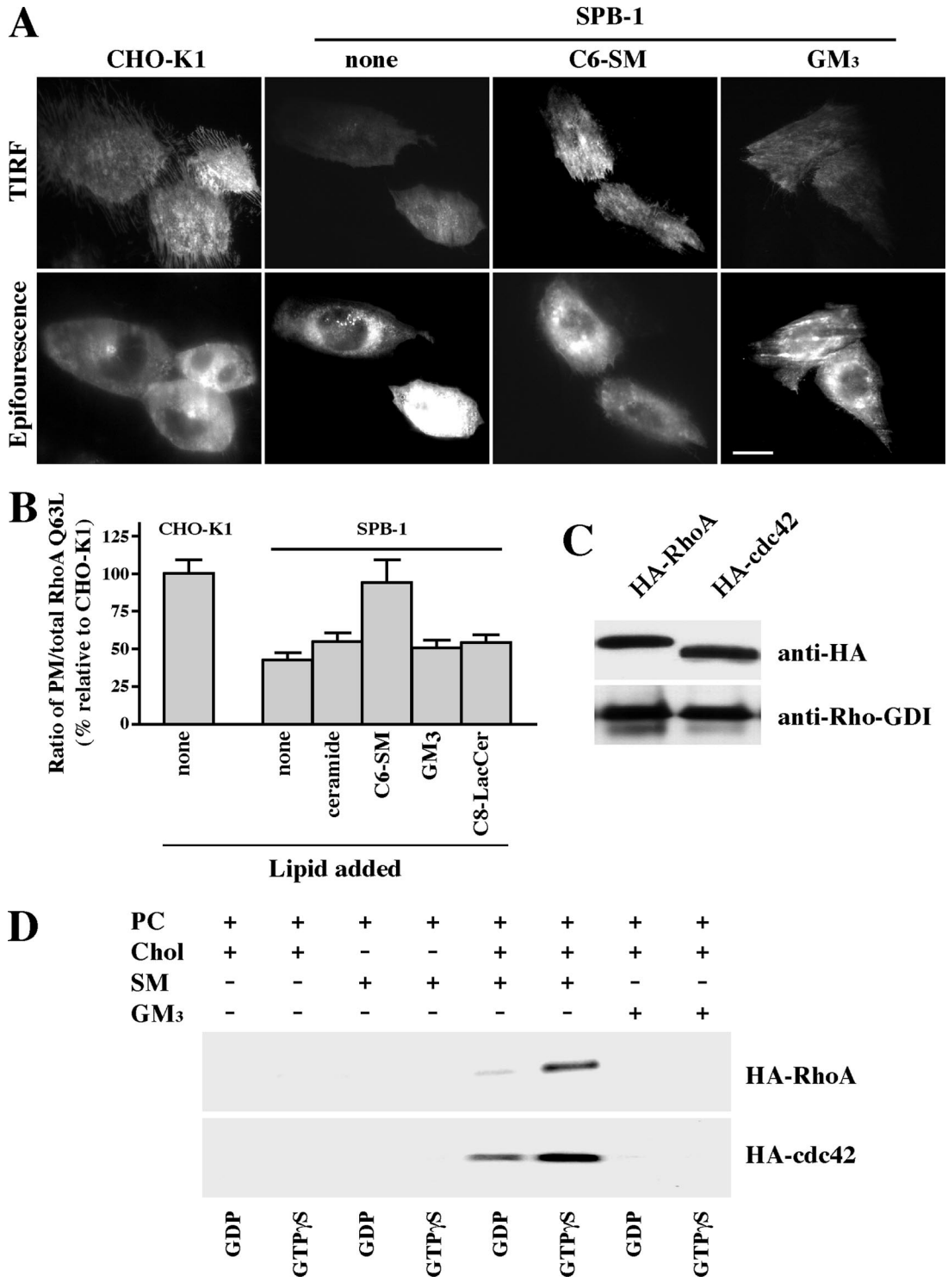


**Figure 7.** Translocation of Rho-GTPases to membranes requires SM. (A andB) CHO-K1 and SPB-1 cells transfected with GFP-RhoA Q63L were cultured under nonpermissive conditions for 48 h and then serum starved. The SPB-1 cells were incubated for 30 min at 10°C ± 20 $\mu$M C6-SM/BSA or $GM_3$/BSA in HMEM and then observed by TIRF or epifluorescence microscopy at 10°C. Bar, 10 $\mu$m. (B) PM-associated GFP-RhoA Q63L fluorescence was quantified relative to total cell fluorescence by image analysis as described in Figure 6E. PM/total cell fluorescence ratios calculated for SBP-1 cells ± lipids are expressed relative to the PM/total ratio in CHO-K1 cells (with no added lipid), which was set to 100. Values are the mean ± SD from ≥50 cells for each condition. (C) CHO-K1 cells were transiently transfected with HA-RhoA or HA-Cdc42. After 48 h, the HA-tagged proteins in the cell lysate were immunoprecipitated using immobilized anti-HA antibody matrix. The immunoprecipitates were analyzed by Western blotting using anti-HA or anti-Rho-GDI antibodies. (D) MLVs were prepared from DMPC/Chol (85/15, mol/mol); DMPC/SM (85/15, mol/mol), DMPC/SM/Chol (42.5/42.5/15, mol/mol/mol), or DMPC/GM3/Chol (42.5/42.5/15, mol/mol/mol) and subsequently incubated with HA-tagged RhoA or Cdc42 in the presence of GDP or GTP$\gamma$S. After washing the MLVs, binding was determined by SDS-PAGE and Western blotting (see *Materials and Methods*).

experiments using the constitutively active, GTP-bound form of RhoA showed that overexpression of this construct in SPB-1 or FB1-treated CHO-K1 cells was unable to restore albumin uptake (our unpublished data). Thus, although active RhoA and Cdc42 are required, they are not sufficient for the endocytosis of albumin, IL-2R, and dextran in SL-depleted cells.

To test the effect of SL depletion on the membrane targeting of endogenous RhoA or Cdc42, particulate and cytosolic fractions were prepared from control, FB1-, or NB-DGJ–treated cells by subcellular fractionation (del Pozo *et al*., 2004). Western blotting showed that both RhoA and Cdc42 translocated to the membrane fraction in control and NB-DGJ–treated cells after serum stimulation, but little translocation to the membrane fraction was seen in FB1-treated cells (Figure 6, A–C). This indicates that a subgroup of SLs, but not GSLs, are critical for membrane targeting of RhoA and Cdc42.

We also evaluated the effect of SL depletion on RhoA and Cdc42 targeting to the PM in living cells. SPB-1 and CHO-K1 cells were transfected with the GFP fusion protein of constitutively active forms of either RhoA or Cdc42 (GFP-RhoA Q63L or GFP-Cdc42 Q61L). GFP fluorescence at the PM was visualized using TIRF microscopy, whereas the total cell-associated fluorescence was assessed by epifluorescence. TIRF microscopy demonstrated that GFP-RhoA Q63L and GFP-Cdc42 Q61L fluorescence at the PM was greatly reduced in SPB-1 cells grown at the nonpermissive temperature relative to CHO-K1 cells (Figure 6D, left), whereas epifluorescence images of the same cells (Figure 6D, right) demonstrated that the total fluorescence present in these cells was approximately the same. Thus, despite their constitutively activated status, the proportion of RhoA Q63L and Cdc42 Q61L at the PM was greatly reduced in SPB-1 cells at the nonpermissive temperature relative to CHO-K1 cells (Figure 6, D and E). SPB-1 cells grown at the permissive temperature exhibited PM/total ratios for RhoA Q63L, and Cdc42 Q61L similar to those seen in CHO-K1 cells (Figure 6E). These findings are in agreement with our studies of membrane targeting of endogenous RhoA and Cdc42 as assessed by cell fractionation (Figure 6, A–C), and suggest that certain SLs are required for translocation of these Rho GTPases to the PM.

Because C6-SM partially restored the uptake of albumin and dextran in SL-depleted cells (Figure 4), we reasoned that it might do so by restoring membrane targeting of RhoA or Cdc42. To test this, SPB-1 cells transfected with GFP-RhoA Q63L were preincubated with exogenous SLs for 30 min at 10°C before examining the distribution of GFP-RhoA in the cells. All steps, including observation under the fluorescence microscope, were carried out at 10°C to minimize formation of SL metabolites. Incubation of SPB-1 cells with C6-SM significantly increased the proportion of GFP-RhoA Q63L at the PM, whereas other lipids such as ceramide, $GM_3$, and C8-LacCer had little effect (Figure 7, A and B). Similar results were obtained using SPB-1 cells expressing GFP-Cdc42 Q61L (our unpublished data). Thus, in combination with the data in Figure 4, these results suggest that SM is the key SL required by RhoA and Cdc42 for regulation of IL-2 and fluid phase endocytosis.

We also studied the in vitro binding of purified RhoA or Cdc42 proteins to artificial MLVs of various compositions. HA-tagged Rho proteins were purified by immunoprecipitation using cell lysates from CHO cells overexpressing HA-RhoA or HA-Cdc42 (see *Materials and Methods*). Endogenous Rho-GDI was also present in the immunoprecipitates (Figure 7C), in agreement with a previous report that RhoA and Cdc42 form a complex with Rho-GDI in cytosolic fractions (Fukumoto *et al*., 1990). The RhoA/RhoGDI or Cdc42/Rho-GDI complexes were loaded with GDP or GTP$\gamma$S and then incubated (30 min at 30°C) with MLVs containing various combinations of phosphatidylcholine (PC), cholesterol, SM, and $GM_3$. The MLVs were then centrifuged, washed, and the bound proteins were examined by SDS-PAGE and Western blotting. MLVs containing PC, cholesterol, and SM showed a strong binding to RhoA or Cdc42 which was enhanced by GTP$\gamma$S, and which was not observed in MLVs lacking cholesterol or containing $GM_3$ in place of SM (Figure 7D); Rho-GDI was not dectectable in any of the MLVs after incubation with the immunoprecipitated proteins (our unpublished data). These results suggest that SM and cholesterol are both crucial for RhoA or Cdc42 binding to membranes.

## DISCUSSION

In the current study, we examined the role of SLs in regulating three separate clathrin-independent endocytic mechanisms in CHO cells. These endocytic mechanisms were shown to be distinct in terms of their cargo and sensitivity to biochemical inhibitors and DN proteins, and they were found to require SLs for proper function. First, we showed that each form of clathrin-independent endocytosis was inhibited by general depletion of SLs whereas clathrin-dependent endocytosis was unaffected under the same conditions. Second, we found that depletion of GSLs, a subgroup of SLs, selectively blocked caveolar-uptake of BODIPY-LacCer, but that it had no effect on the internalization of albumin and IL-2R, and dextran, which are internalized via nonclathrin mechanisms regulated by RhoA and Cdc42, respectively. Inhibition of caveolar endocytosis was accompanied by a decrease in Cav1 at the PM and a reduction in the number of 50- to 80-nm-diameter vesicles at the cell surface. Both cell surface caveolae and caveolar endocytosis could restored by incubation with exogenous GSLs (but not other SLs). Finally, we found that the inhibitory effects of general SL depletion on RhoA- and Cdc42-dependent endocytosis were a result of a requirement of SM for RhoA and Cdc42 translocation to the membrane. Inhibition of these endocytic pathways could be partially reversed by incubating cells with exogenous SM; however, no restoration was seen using exogenous GSLs or ceramide. Together, these results provide the first evidence that SLs differentially regulate multiple clathrin-independent endocytic mechanisms. Below we discuss several points related to these findings.

One potential explanation for our findings is that inhibition of SL or GSL synthesis might result in the accumulation of a lipid second messenger (e.g., ceramide, sphingosine, or sphingosine-phosphate), which in turn modulates selected mechanisms of endocytosis. Indeed, sphingoid base synthesis is required for endocytosis in yeast (Zanolari *et al*., 2000) and ceramide has been shown to modulate endocytosis in mammalian cells (Chen *et al*., 1995; Zha *et al*., 1998). However, several results from the current study suggest that SL second messengers are probably not responsible for the effects on endocytosis reported here. First, a similar inhibition of all three nonclathrin pathways was seen whether SL depletion was accomplished using SPB-1 cells or by FB1 treatment of CHO-K1 cells. FB1 treatment prevents the formation of ceramides, SM, and GSLs (Supplemental Figure 1), but it may cause the accumulation of sphingoid bases (e.g., sphingosine and sphingosine-1-P), whereas SPB-1 cells are not able to synthesize either sphingoid bases or other SLs derived from them. The similar inhibition of nonclathrin endocytic pathways seen in SPB-1 cells or in FB1 treated CHO-K1 cells suggests that these effects are more likely

because of the loss of required higher order SLs than to the accumulation of sphingoid bases. In addition, we showed that addition of exogenous GSLs or SM (but not ceramide) could partially restore caveolar and Rho-dependent endocytosis, respectively, suggesting specific roles for higher order SLs in these endocytic processes (Figure 4C).

### *GSL Requirement for Caveolar Endocytosis*

Previous studies from our laboratory have shown that a fluorescent analog of LacCer is internalized almost exclusively via caveolae in multiple cell types, including CHO-K1 cells (Sharma *et al*., 2003; Singh *et al*., 2003). Evidence for this internalization mechanism comes from the initial colocalization of LacCer with other caveolar markers and with Cav1-fluorescent proteins and from the use of pharmacological inhibitors known to preferentially block this pathway. In the current study, we showed a specific requirement of GSLs for caveolar endocytosis because only this pathway was disrupted by PPPP or NB-DGJ, two inhibitors of GSL synthesis (refer to Supplemental Figure 1). Unfortunately, other markers for caveolar endocytosis in CHO cells, apart from BODIPY-LacCer, are not available. For example, although albumin is endocytosed via caveolae in other cell types (Schnitzer *et al*., 1994; Minshall *et al*., 2002; Singh *et al*., 2003; Sharma *et al*., 2004), in CHO cells fluorescent albumin internalized via the RhoA-dependent pathway, similar to the IL-2R, and it did not colocalize with Cav1-mRed or BODIPY-LacCer upon internalization (Supplemental Table 2). The reason that albumin is endocytosed by a noncaveolar mechanism in CHO cells is unknown but may reflect a different distribution of albumin binding protein(s) at the surface of CHO cells versus other cell types. A second potential marker for caveolar uptake is CtxB (Henley *et al*., 1997; Orlandi and Fishman, 1998; Singh *et al*., 2003); however, this toxin binds to $GM_1$ ganglioside, which is not detectable in CHO-K1 cells.

Interestingly, inhibition of GSL synthesis also reduced Cav1 at the PM and decreased the number of 50- to 80-nm-diameter vesicles connected with the cell surface (Figure 5). Such vesicles are consistent with the reported size and shape of caveolae. These data suggest that the reduction in caveolar endocytosis observed upon GSL depletion occurs because GSLs are required for the PM organization of caveolae. The present findings are in apparent contrast to a previous report in which caveolae structure and sorting of caveolin were found to be normal in NIH-3T3 cells after treatment with PPPP (Shu *et al*., 2000). This discrepancy could be because of differences in the cell types used. For example, differing endogenous lipid compositions in different cell types could have differential effects on the organization of caveolae. Another important difference between the studies is that for immunofluorescence we used permeabilization and fixation conditions and selective antibodies to differentially stain PM versus intracellular (e.g., Golgi) Cav1, unlike the technique used by Shu *et al*. (2000), which broadly stained Cav1. In addition, for EM studies cells were coated with ruthenium red so that we could selectively identify surface-connected smooth vesicles (e.g., caveolae), whereas Shu *et al*. (2000) apparently used only size and proximity to the PM as a means to identify caveolae. Thus, our morphological methods may have been more sensitive for detecting a loss of caveolae from the PM. Most importantly, we showed that treatment with PPPP or NB-DGJ caused a loss of caveolar endocytosis, a feature that was not monitored in the Shu study. In addition, we could restore cell surface caveolae and caveolar endocytosis by incubating GSL depleted cells with exogenous GSLs (e.g., $GM_3$ ganglioside or nonfluorescent LacCer), whereas no restoration was seen when exogenous SM or ceramide were used (Figures 4C and 5, C and D).

### *Sphingomyelin Is Required for Rho GTPase-dependent Mechanisms of Endocytosis*

The two Rho dependent-pathways used for endocytosis of IL-2R (RhoA) and dextran (Cdc42) were also inhibited by general SL depletion but not by inhibitors of GSL synthesis (Figure 3). Importantly, endocytosis by the Rho-dependent pathways in SL-depleted cells could be restored by addition of exogenous SM (but not exogenous GSLs or ceramide) (Figure 4). Furthermore, hydrolysis of SM at the cell surface with SMase inhibited both RhoA- and Cdc42-dependent uptake (Supplemental Table 1). Together, these results suggest a specific requirement for SM in endocytosis via the RhoA- and Cdc42-dependent pathways.

To study the mechanism by which RhoA- and Cdc42-mediated processes might be affected by SLs, we first examined their GTP loading in control, FB1-, or NB-DGJ–treated cells and found that SL depletion using either inhibitor did not affect the activation of these Rho GTPases (Supplemental Figure 6). Also, overexpression of the GTP bound form of RhoA was not able to restore the endocytosis of albumin in SPB-1 cells (our unpublished data), further indicating that GTP loading was not involved.

We next studied the targeting of RhoA and Cdc42 to membranes because several studies have shown that upon activation, Rho GTPases are targeted to specific membrane microdomains where they are coupled to their effectors and trigger downstream signaling events (del Pozo *et al*., 2004; Palazzo *et al*., 2004). Using subcellular fractionation we found that targeting of RhoA and Cdc42 to membranes was reduced >70% in FB1-treated cells compared with control cells (Figure 6, A–C). In addition, TIRF microscopy demonstrated that in SPB-1 cells transfected with GFP fusion proteins of RhoA Q63L or Cdc42 Q61L, there was a dramatic decrease in GFP fluorescence at the PM compared with CHO-K1 cells (Figure 6, D and E). Importantly, PM targeting of GFP-RhoA (Figure 7, A and B) and -Cdc42 (our unpublished data) could be partially restored by incubating cells with SM but not with exogenous ceramide, $GM_3$, or LacCer (Figure 7B). Finally, we showed that membrane targeting of RhoA and Cdc42 could be recapitulated in vitro using artificial lipid vesicles (liposomes) of defined composition (Figure 7D). Interestingly, this association occurred only when both SM and cholesterol were present in the liposomes.

Although our results provide strong evidence that SM is essential for the membrane targeting of RhoA and Cdc42, they also pose an intriguing topological problem. Namely, how does SM, which is highly enriched in the external leaflet of PM bilayer (Pagano, 1988; Futerman *et al*., 1990; van Echten and Sandhoff, 1993; Sprong *et al*., 2001), interact with Rho GTPases on the inner leaflet of the PM? One possibility is that the two leaflets of the bilayer are "coupled" such that changes in composition on one side of the membrane induce changes in the structure, composition, or organization on the opposite leaflet. "Bilayer coupling" at the PM has been observed for H- and K-ras and for GFP modified with various lipid anchors (Prior *et al*., 2001; Zacharias *et al*., 2002). Our results showing that both SM and cholesterol were required for the binding of RhoA and Cdc40 to lipid vesicles suggest the possibility that SM might contribute to the organization of cholesterol on the inner leaflet of the PM into microdomains for which the Rho proteins have an affinity. Alternatively, it is possible that there is a small pool of SM on the cytosolic leaflet of the PM as has been reported previously (Linardic and Hannun, 1994; Andrieu *et al*., 1996), which is

not readily detected but plays a key role in binding RhoA and Cdc42. Future studies and new methodologies will be required to distinguish between these alternatives.

In summary, the current study demonstrates that SLs can selectively regulate clathrin-independent mechanisms of endocytosis and helps to further define the critical components necessary for these different uptake mechanisms. Our data also provides further evidence that caveolar endocytosis and other nonclathrin uptake mechanisms are distinct processes.

## ACKNOWLEDGMENTS

This work was supported by Public Health Service Grant GM-22942 (to R.E.P.). D.K.S. was supported by a Mayo-Kendall Fellowship.

## REFERENCES

Andrieu, N., Salvayre, R., and Levade, T. (1996). Comparative study of the metabolic pools of sphingomyelin and phosphatidylcholine sensitive to tumor necrosis factor. Eur. J. Biochem. *236*, 738–745.

Bain, J., McLauchlan, H., Elliott, M., and Cohen, P. (2003). The specificities of protein kinase inhibitors: an update. Biochem. J. *371*, 199–204.

Bito, R., Hino, S., Baba, A., Tanaka, M., Watabe, H., and Kawabata, H. (2005). Degradation of oxidative stress-induced denatured albumin in rat liver endothelial cells. Am. J. Physiol. *289*, C531–C542.

Brown, D. A., and London, E. (1998). Functions of lipid rafts in biological membranes. Annu. Rev. Cell Dev. Biol. *14*, 111–136.

Chen, C.-S., Rosenwald, A. G., and Pagano, R. E. (1995). Ceramide as a modulator of endocytosis. J. Biol. Chem. *270*, 13291–13297.

Choudhury, A., Dominguez, M., Puri, V., Sharma, D. K., Narita, K., Wheatley, C. W., Marks, D. L., and Pagano, R. E. (2002). Rab proteins mediate Golgi transport of caveola-internalized glycosphingolipids and correct lipid trafficking in Niemann-Pick C cells. J. Clin. Investig. *109*, 1541–1550.

Damm, E. M., Pelkmans, L., Kartenbeck, J., Mezzacasa, A., Kurzchalia, T., and Helenius, A. (2005). Clathrin- and caveolin-1-independent endocytosis: entry of simian virus 40 into cells devoid of caveolae. J. Cell Biol. *168*, 477–488.

del Pozo, M. A., Alderson, N. B., Kiosses, W. B., Chiang, H. H., Anderson, R. G., and Schwartz, M. A. (2004). Integrins regulate Rac targeting by internalization of membrane domains. Science *303*, 839–842.

Duncan, M. J., Shin, J. S., and Abraham, S. N. (2002). Microbial entry through caveolae: variations on a theme. Cell Microbiol. *4*, 783–791.

Fukumoto, Y., Kaibuchi, K., Hori, Y., Fujioka, H., Araki, S., Ueda, T., Kikuchi, A., and Takai, Y. (1990). Molecular cloning and characterization of a novel type of regulatory protein (GDI) for the rho proteins, ras p21-like small GTP-binding proteins. Oncogene *5*, 1321–1328.

Futerman, A. H., Stieger, B., Hubbard, A. L., and Pagano, R. E. (1990). Sphingomyelin synthesis in rat liver occurs predominantly at the cis and medial cisternae of the Golgi apparatus. J. Biol. Chem. *265*, 8650–8657.

Gauthier, N. C., Monzo, P., Kaddai, V., Doye, A., Ricci, V., and Boquet, P. (2005). Helicobacter pylori VacA cytotoxin: a probe for a clathrin-independent and Cdc42-dependent pinocytic pathway routed to late endosomes. Mol. Biol. Cell *16*, 4852–4866.

Hanada, K., Nishijima, M., and Akamatsu, Y. (1990). A temperature-sensitive mammalian cell mutant with thermolabile serine palmitoyltransferase for the sphingolipid biosynthesis. J. Biol. Chem. *265*, 22137–22142.

Hanke, J. H., Gardner, J. P., Dow, R. L., Changelian, P. S., Brissette, W. H., Weringer, E. J., Pollok, B. A., and Connelly, P. A. (1996). Discovery of a novel, potent, and Src family-selective tyrosine kinase inhibitor. Study of Lck- and FynT-dependent T cell activation. J. Biol. Chem. *271*, 695–701.

Henley, J., Krueger, E., Oswald, B., and McNiven, M. (1997). Dynamin-mediated internalization of caveolae in mammalian cells. Mol. Biol. Cell *8* (suppl), 425a.

Henley, J. R., Krueger, E. W., Oswald, B .J., and McNiven, M. A. (1998). Dynamin-mediated internalization of caveolae. J. Cell Biol. *141*, 85–99.

Johannes, L., and Lamaze, C. (2002). Clathrin-dependent or not: is it still the question? Traffic *3*, 443–451.

John, T. A., Vogel, S. M., Tiruppathi, C., Malik, A. B., and Minshall, R. D. (2003). Quantitative analysis of albumin uptake and transport in the rat microvessel endothelial monolayer. Am. J. Lung Cell Mol. Physiol. *284*, L187–L196.

Kirkham, M., Fujita, A., Chadda, R., Nixon, S. J., Kurzchalia, T. V., Sharma, D. K., Pagano, R. E., Hancock, J. F., Mayor, S., and Parton, R. G. (2005b). Ultrastructural identification of uncoated caveolin-independent early endocytic vehicles. J. Cell Biol. *168*, 465–476.

Lamaze, C., Dujeancourt, A., Baba, T., Lo, C. G., Benmerah, A., and Dautry-Varsat, A. (2001). Interleukin 2 receptors and detergent-resistant membrane domains define a clathrin-independent endocytic pathway. Mol. Cell *7*, 661–671.

Le, P. U., and Nabi, I. R. (2003). Distinct caveolae-mediated endocytic pathways target the Golgi apparatus and the endoplasmic reticulum. J. Cell Sci. *116*, 1059–1071.

Lee, L., Abe, A., and Shayman, J. A. (1999). Improved inhibitors of glucosylceramide synthase. J. Biol. Chem. *274*, 14662–14669.

Lencer, W. I., Hirst, T. R., and Holmes, R. K. (1999). Membrane traffic and the cellular uptake of cholera toxin. Biochim. Biophys. Acta *1450*, 177–190.

Linardic, C. M., and Hannun, Y. A. (1994). Identification of a distinct pool of sphingomyelin involved in the sphingomyelin cycle. J. Biol. Chem. *269*, 23530–23537.

Marjomaki, V., Pietianinen, V., Matilainen, H., Upla, P., Ivaska, J., Nissinen, L., Reunanen, H., Huttunen, P., Hyypia, T., and Heino, J. (2002). Internalization of echovirus 1 in caveolae. J. Virol. *76*, 1856–1865.

Martin, O. C., and Pagano, R. E. (1994). Internalization and sorting of a fluorescent analog of glucosylceramide to the Golgi apparatus of human skin fibroblasts: utilization of endocytic and nonendocytic transport mechanisms. J. Cell Biol. *125*, 769–781.

Merrill, J., A. H., Liotta, D. C., and Riley, R. T. (1996). Fumonisins: fungal toxins that shed light on sphingolipid function. Trends Cell Biol. *6*, 218–223.

Mineo, C., and Anderson, G. W. (2001). Potocytosis. Histochem. Cell Biol. *116*, 109–118.

Minshall, R. D., Tiruppathi, C., Vogel, S. M., and Malik, A. B. (2002). Vesicle formationi and trafficking in endothelial cells and regulation of endothelial barrier function. Histochem. Cell Biol. *117*, 105–112.

Nabi, I. R., and Le, P. U. (2003). Caveolae/raft-dependent endocytosis. J. Cell Biol. *161*, 673–677.

Nichols, B. J., and Lippincott-Schwartz, J. (2001). Endocytosis without clathrin coats. Trends Cell Biol. *11*, 406–412.

Norkin, L. C. (2001). Caveolae in the uptake and targeting of infectious agents and secreted toxins. Adv. Drug Deliv. Rev. *49*, 301–315.

Orlandi, P. A., and Fishman, P. H. (1998). Filipin-dependent inhibition of cholera toxin: evidence for toxin internalization and activation through caveolae-like domains. J. Cell Biol. *141*, 905–915.

Pagano, R. E. (1988). What is the fate of diacylglycerol produced at the Golgi apparatus? Biochem. Sci. *13*, 202–205.

Palazzo, A. F., Eng, C. H., Schlaepfer, D. D., Marcantonio, E. E., and Gundersen, G. G. (2004). Localized stabilization of microtubules by integrin- and FAK-facilitated Rho signaling. Science *303*, 836–839.

Parton, R. G. (2003). Caveolae–from ultrastructure to molecular mechanisms. Nat. Rev. Mol. Cell. Biol. *4*, 162–167.

Parton, R. G., and Richards, A. A. (2003). Lipid rafts and caveolae as portals for endocytosis: new insights and common mechanisms. Traffic *4*, 724–738.

Patel, H. K., Willhite, D. C., Patel, R. M., Ye, D., Williams, C. L., Torres, E. M., Marty, K. B., MacDonald, R. A., and Blanke, S. R. (2002). Plasma membrane cholesterol modulates cellular vacuolation induced by the *Helicobacter pylori* vacuolating cytotoxin. Infect. Immun. *70*, 4112–4123.

Pelkmans, L., Kartenbeck, J., and Helenius, A. (2001). Caveolar endocytosis of simian virus 40 reveals a new two-step vesicular-transport pathway to the ER. Nat. Cell Biol. *3*, 473–483.

Pelkmans, L., Püntener, D., and Helenius, A. (2002). Local actin polymerization and dynamin recruitment in SV40-induced internalization of caveolae. Science *296*, 535–539.

Platt, F. M., Neises, G. R., Karlsson, G. B., Dwek, R. A., and Butters, T. D. (1994). N-Butyldeoxygalactonojirimycin inhibits glycolipid biosynthesis but does not affect N-linked oligosaccharide processing. J. Biol. Chem. *269*, 27108–27114.

Pol, A., Martin, S., Fernandez, M. A., Ingelmo-Torres, M., Ferguson, C., Enrich, C., and Parton, R. G. (2005). Cholesterol and fatty acids regulate dynamic caveolin trafficking through the Golgi complex and between the cell surface and lipid bodies. Mol. Biol. Cell *16*, 2091–2105.

Prior, I. A., Harding, A., Yan, J., Sluimer, J., Parton, R. G., and Hancock, J. F. (2001). GTP-dependent segregation of H-ras from lipid rafts is required for biological activity. Nat. Cell Biol. *3*, 368–375.

Puri, V., Jefferson, J. R., Singh, R. D., Wheatley, C. L., Marks, D. L., and Pagano, R. E. (2003). Sphingolipid storage induces accumulation of intracellular cholesterol by stimulating SREBP-1 cleavage. J. Biol. Chem. *278*, 20961–20970.

Puri, V., Watanabe, R., Singh, R. D., Dominguez, M., Brown, J. C., Wheatley, C. L., Marks, D. L., and Pagano, R. E. (2001). Clathrin-dependent and -independent internalization of plasma membrane sphingolipids initiates two Golgi targeting pathways. J. Cell Biol. *154*, 535–547.

Richterova, Z., Liebl, D., Horak, M., Palkova, Z., Stokrova, J., Hozak, P., Korb, J., and Forstova, J. (2001). Caveolae are involved in the trafficking of mouse polyomavirus virions and artificial VP1 pseudocapsids toward cell nuclei. J. Virol. *75*, 10880–10891.

Sabharanjak, S., Sharma, P., Parton, R. G., and Mayor, S. (2002). GPI-anchored proteins are delivered to recycling endosomes via a distinct cdc42-regulated, clathrin-independent pinocytic pathway. Dev. Cell *2*, 411–423.

Schnitzer, J. E., and Oh, P. (1994). Albondin-mediated capillary permeability to albumin. Differential role of receptors in endothelial transcytosis and endocytosis of native and modified albumins. J. Biol. Chem. *269*, 6072–6082.

Schnitzer, J. E., Oh, P., Pinney, E., and Allard, J. (1994). Filipin-sensitive caveolae-mediated transport in endothelium: reduced transcytosis, scavenger endocytosis, and capillary permeability of select macromolecules. J. Cell Biol. *127*, 1217–1232.

Sharma, D. K., Brown, J. C., Cheng, Z., Holicky, E. L., Marks, D. L., and Pagano, R. E. (2005). The glycosphingolipid, lactosylceramide, regulates beta1 -integrin clustering and endocytosis. Cancer Res. *65*, 8233–8241.

Sharma, D. K., Brown, J. C., Choudhury, A., Peterson, T. E., Holicky, E., Marks, D. L., Simari, R., Parton, R. G., and Pagano, R. E. (2004). Selective stimulation of caveolar endocytosis by glycosphingolipids and cholesterol. Mol. Biol. Cell *15*, 3114–3122.

Sharma, D. K., Choudhury, A., Singh, R. D., Wheatley, C. L., Marks, D. L., and Pagano, R. E. (2003). Glycosphingolipids internalized via caveolar-related endocytosis rapidly merge with the clathrin pathway in early endosomes and form microdomains for recycling. J. Biol. Chem. *278*, 7564–7572.

Shin, J.-S., Gao, Z., and Abraham, N. (2000). Involvement of cellular caveolae in bacterial entry into mast cells. Science *289*, 785–788.

Shu, L., Lee, L., Chang, Y., Holzman, L. B., Edwards, C. A., Shelden, E., and Shayman, J. A. (2000). Caveolar sructure and protein sorting are maintained in NIH 3T3 cells independent of glycosphingolipid depletion. Arch. Biochem. Biophys. *373*, 83–90.

Simons, K., and Vaz, W. L. (2004). Model systems, lipid rafts, and cell membranes. Annu. Rev. Biophys. Biomol. Struct. *33*, 269–295.

Singh, R. D., Puri, V., Valiyaveettil, J. T., Marks, D. L., Bittman, R., and Pagano, R. E. (2003). Selective caveolin-1-dependent endocytosis of glycosphingolipids. Mol. Biol. Cell *14*, 3254–3265.

Smart, E., Graf, G., McNiven, M., Sessa, W., Elgelman, J., Scherer, P., Okamoto, T., and Lisanti, M. (1999). Caveolins, liquid-ordered domains, and signal transduction. Mol. Cell Biol. *19*, 7289–7304.

Sprong, H., van der Sluijs, P., and van Meer, G. (2001). How proteins move lipids and lipids move proteins. Mol. Cell Biol. *2*, 504–513.

Torgersen, M. L., Skretting, G., van Deurs, B., and Sandvig, K. (2001). Internalization of cholera toxin by different endocytic mechanisms. J. Cell Sci. *114*, 3737–3742.

van Echten, G., and Sandhoff, K. (1993). Ganglioside metabolism. Enzymology, Topology, and regulation. J. Biol. Chem. *268*, 5341–5344.

Zacharias, D. A., Violin, J. D., Newton, A. C., and Tsien, R. Y. (2002). Partitioning of lipid-modified monomeric GFPs into membrane microdomains of live cells. Science *296*, 913–916.

Zanolari, B., Friant, S., Funato, K., Sutterlin, C., Stevenson, B. J., and Riezman, H. (2000). Sphingoid base synthesis requirement for endocytosis in *Saccharomyces cerevisiae*. EMBO J. *19*, 2824–2833.

Zha, X., Pierini, L. M., Leopold, P. L., Skiba, P. J., Tabas, I., and Maxfield, F. R. (1998). Sphingomyelinase treatment induces ATP-independent endocytosis. J. Cell Biol. *140*, 39–47.